Progress In Electromagnetics Research, Vol. 109, 245–262, 2010

LIMITATIONS OF APPROXIMATIONS TOWARDS FOURIER OPTICS FOR INDOOR ACTIVE MILLIMETER WAVE IMAGING SYSTEMS

F. Qi, V. Tavakol, D. Schreurs, and B. Nauwelaers

Division ESAT-TELEMIC, Katholieke Universiteit Leuven
Kasteelpark Arenberg 10, Leuven-Heverlee 3001, Belgium

Abstract—To simulate imaging systems, Fourier optics has been applied very successfully to optics for decades. However, when simply moving to indoor millimeter wave imaging systems, some assumptions underlying the Fourier optics may break down, which contribute to the errors by applying Fourier optics. During the review of mathematical derivation of the Fourier optics, we point out how the errors are introduced by making the Fresnel approximation and omitting the phase factors. To distinguish from much literature, we discuss the accuracy of Fresnel approximation rather than plane wave. Moreover, we check the simulation results for millimeter wave imaging systems working in both pixel scanning mode and focal plane array mode and compare them to the results predicted by Fourier optics. It is shown that the difference can be 28% for the speckle contrast when the object is with certain roughness. The optical routine is that when the lens is four times' larger than the object, the imaging system can be considered as isoplanatic, thus Fourier optics can hold. Our simulation results imply that it may not be valid in indoor millimeter wave imaging systems. The goal of this paper is to draw some attention to the possibly large errors when modeling or designing the indoor millimeter wave imaging systems by Fourier optics directly. The mathematical discussions of the inaccuracies due to some approximations in Fourier optics can serve to understand and deal with aberrations.

Received 5 August 2010, Accepted 15 October 2010, Scheduled 23 October 2010
Corresponding author: F. Qi (feng.qi@esat.kuleuven.be).

1. INTRODUCTION

In Fourier optics, imaging is considered as a linear spatial invariant process with a corresponding impulse response called "amplitude transfer function" defined by the optical pupil [1]. Consequently, linear system theory holds. Due to the elegant mathematical expression of this approach and ease of calculations by Fast Fourier Transform (FFT), it is widely applied to simulate various kinds of optical imaging systems, including human vision [2] and photolithography [3]. On the other end of the spectrum, researchers in microwave imaging are influenced by this concept as well. Recently, millimeter wave imaging is becoming more and more important in the areas of public security and industrial detection, since waves in this frequency band allow both good resolution and penetration ability [4]. Based on Fourier optics, simulations are implemented for both active [5] and passive systems at 100 GHz [6]. The question is how accurate the method can be in such cases. We will show how the assumptions made during the mathematical derivation of the Fourier relationship lead to possibly large errors in case of coherent millimeter wave imaging. Due to the cost of the component at millimeter wave frequencies, in most labs, studies of focal plane array imaging generally originate from prototypes which work in the pixel scanning mode. We will prove that the imaging array setup is more than a parallel realization of the pixel scanning system, while the illuminated area plays an important role.

This paper is structured as follows: in Section 2, we compare the different imaging properties between optical and millimeter wave imaging systems. Next, we briefly reviewed the derivation of Fourier optics. In Section 4, we compare the imaging results for both smooth and rough objects based on Fourier optics and the scalar diffraction model. In Section 5, we analyze the accuracy of the Fresnel approximation and the influence of the quadratic phase factor by stationary phase method and spectrum analysis respectively. The two points above contribute to the inaccuracies due to approximations towards Fourier optics, which can be large in case of indoor millimeter wave imaging systems. Moreover, the two sections above help to explain the imaging results in Section 4. In the end, we will come to conclusions in Section 6.

2. COMPARISON BETWEEN OPTICAL AND MILLIMETER WAVE IMAGING SYSTEMS

Either optical or millimeter wave imaging can be considered as an information transmission process, and the lens provides a channel. In

practice, we can only sense certain parts of the object, whose radiations are captured by our lenses and projected to sensors. Fast phase shift corresponds to roughness of the object physically, while from the wave optics point of view, it leads to large diffraction angles. In Figure 1, we conclude the imaging process in four cases. When the object is flat, wave propagates in a paraxial manner. Geometrical optics (GO) works well in this case. In optical imaging systems, generally we are interested at electrically large features and we use line (1) to represent this case. As the spatial frequency goes higher, diffraction angle becomes larger. For line (2), the diffracted beams can still be captured by lens' aperture. In this case, it is possible to recover the image with high fidelity once the aberration problem can be solved. However, for lenses with small f-numbers, aberration is a challenging problem. When the spatial frequency of a certain part of objects is high enough, as line (3) shows, large diffraction angles generate escaping beams and a dark spot will appear on image plane. For those parts with extremely high spatial frequency components, evanescent waves can be generated, as shown by line (4). The information is totally lost in this case.

There are five reasons which contribute to the success of Fourier optics at optical frequencies: first, paraxial condition is usually satisfied (Line 1 in Figure 1), which means that phase errors are small; second, Fraunhofer diffraction is the most important case encountered in engineering optics [7], so that incident field on the lens' aperture can be considered as a simple Fourier transform of the object's field; third, considering the resolution, it is large in terms of electrical size, which means that only the relatively low spatial frequency components gain

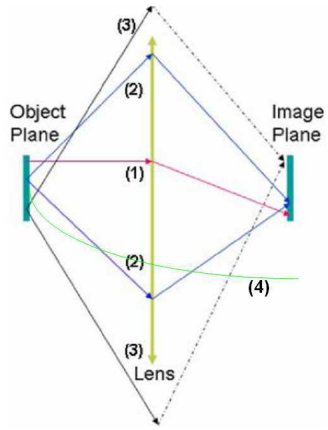

Figure 1. Image formation process.

interest; fourth, there are very good lenses to deal with aberrations, so as to guarantee the isoplanatic condition in a large area; fifth, the illumination is quite flexible, which can help to eliminate the influence of the quadratic phase factor, making the system more isoplanatic [1].

Compared to optical imaging systems, the challenge for millimeter wave imaging systems is to realize higher resolution in terms of electrical size in a more non-paraxial case. In [8], by simply scaling an optical imaging system to a millimeter wave imaging system based on wavelengths, an optical camera would have at millimeter wave frequencies a system scale of hundreds of meters with a lens' diameter of tens of meters. Considering the resolution, it is in the order of tenths of a millimeter for the human eye in the optical case, while the corresponding value for a millimetre wave imaging system would be around ten meters. However, the dimension of practical millimeter wave imaging systems is limited to a few meters for indoor applications, with a resolution of interest at the level of centimetres or even less. In such a compact system, we have to be cautious about the physical size of the object to be imaged and how paraxial it can be. The resolution for a millimeter wave imaging system is generally a few wavelengths. To achieve high resolution considering the wavelength, it is common to apply a lens with a small f-number so as to collect more transmitted or reflected waves within a larger solid angle. For general optical imaging systems, the f-number is 2.5 or larger, while for millimeter wave imaging systems, it is common to be around one, making the wave propagation from lens to image plane not quite paraxial. Moreover, the field-of-view of millimeter wave imaging systems is generally very large, which can be even 60 degrees in contraband detection systems [4]. This requirement is more demanding than most optical imaging systems. Nowadays, at millimeter wave frequencies, the performance of the lens can not compete with optical systems, which means that more significant aberrations can not guarantee a large enough isoplanatic area. Compared to optical lenses, the design work at millimeter frequencies is still very young, which mainly follows the optical routine based on GO, without considering much about millimeter wave features [9, 10]. However, the validity of GO or expanded version of GO is limited to high frequency problems [11, 12]. At millimeter wave frequencies, considering the much smaller electrical size of interested object's features and lens compared to optics, diffraction effects are much more important. Optical lens design is a good starting point, but millimeter wave lens design is more complicated for imaging applications and full-wave calculations should be included. Last but not least, for millimeter wave imaging systems in focal plane array mode, it is common to realize the large-area illumination by expanding

the Gaussian beam, which means that the illumination is not as good as in optics, making the aberration problem more serious.

According to the discussions above, in practical indoor millimeter wave systems which work in the focal plane array imaging mode, we should consider the practical size of the components, dimension of the system and objects with possible roughness. In order to capture more radiations from the object, we hope to decrease the distance between object and lens, while in order to weaken the aberration of the image, we wish to make the distance larger. So trade-offs are required for system design.

3. IMAGING MODEL

The considered imaging system is shown in Figure 2, including three components: an object, a lens and an image plane, with the following denotations: (ξ, η): object plane; (x, y): lens plane; (u, v): image plane; U_o: field distribution on the object plane; U_l: field distribution in front of the lens; U_l': field distribution behind the lens; Z_1: distance between object plane and lens; Z_2: distance between lens and image plane.

According to the scalar diffraction theorem, propagated fields can be calculated by the Rayleigh-Sommerfeld formula (1), where (x, y) and (ξ,η) are the spatial coordinates in two planes of which the latter one is the source plane. Concerning the exponential factor in (1), r is approximated by retaining the first two terms of its binominal expansion. For the denominator part, r is the distance between the two planes, as a constant. Consequently, (1) is approximated by (2),

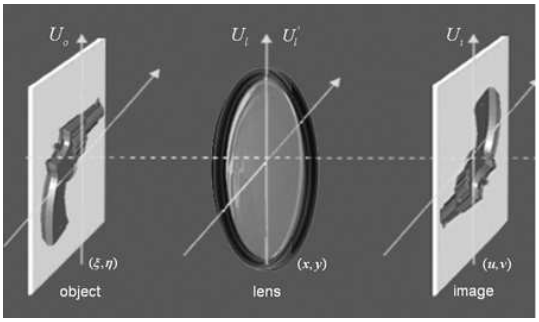

Figure 2. Imaging system setup, which contains an object, a lens and an image plane.

which is called the Fresnel approximation [1].

$$U(x,y)=\frac{z}{j\lambda}\iint U(\xi,\eta)\frac{e^{jkr}}{r^2}d\xi d\eta \tag{1}$$

$$U(x,y)=\frac{e^{jkz}}{j\lambda z}e^{j\frac{k}{2z}(x^2+y^2)}\iint\left[U(\xi,\eta)e^{j\frac{k}{2z}(\xi^2+\eta^2)}\right]e^{-j\frac{2\pi}{\lambda z}(x\xi+y\eta)}d\xi d\eta \tag{2}$$

Essentially, the derivation of Fourier optics is based on two Fresnel approximations in the zone of Z_1 and Z_2, plus a thin lens model as a phase shift component [1]. In this case, the field distribution in the image plane is expressed as in (3), where $P(x,y)$ stands for the aperture of the lens. By deleting all the linear and quadratic phase factors, (3) is casted into (4), in which the Fourier relationship is attained in normalized coordinates considering the amplification ratio. In spatial frequency domain, formula (4) implies a low-pass filtering process.

$$U_i(u,v)=\frac{e^{jkz_1}}{j\lambda z_1}\cdot\frac{e^{jkz_2}}{j\lambda z_2}\cdot e^{j\frac{k}{2z_2}(u^2+v^2)}\times\iint P(x,y)e^{j\frac{k}{2}\left(x^2+y^2\right)\left(\frac{1}{z_1}+\frac{1}{z_2}-\frac{1}{f}\right)}$$
$$\times\left[\iint[U_o(\xi,\eta)e^{j\frac{k}{2z_1}(\xi^2+\eta^2)}]e^{-j\frac{2\pi}{\lambda z_1}(x\xi+y\eta)}d\xi d\eta\right]\times e^{-j\frac{2\pi}{\lambda z_2}(ux+vy)}dxdy \tag{3}$$

$$U_i(u,v)\propto\iint P(x,y)\times\left[\iint U_o(\xi,\eta)e^{-j\frac{2\pi}{\lambda z_1}(x\xi+y\eta)}d\xi d\eta\right]$$
$$\times e^{-j\frac{2\pi}{\lambda z_2}(ux+vy)}dxdy \tag{4}$$

However, we should pay attention to the approximations towards formula (4), which essentially implies a Fraunhofer approximation between object and lens plus a Fresnel approximation between lens and image plane. In [13], the omission of quadratic phase factor which interacts with the object field directly, is the key to change the kernel as pulse response from spatial variant to spatial invariant. This is often called "isoplanatic" and it requires a very large distance (infinite theoretically) between object and lens, which matches our discussions of the Fraunhofer diffraction condition above. Tichenor pointed out that this requirement can be loosened and the imaging model can be applied if the size of the object does not exceed one-fourth of the linear dimension of the lens' aperture [14].

4. IMAGING RESULTS COMPARISON

In this section, we will compare Fourier optics, as described by Formula (4) to another model, which is based on Rayleigh-Sommerfeld diffraction in [15]. Moreover, the influence of illuminated area will be shown. Considering the huge electrical size of the millimeter

wave imaging system, it is extremely difficult to implement full-wave calculations at the system level by the computer nowadays. Thus, system simulations based on scalar diffraction can be considered as a good tradeoff between accuracy and calculation speed. More advanced algorithms for electromagnetic scattering can be found in [16–23].

In a millimeter wave imaging system that works in pixel scanning mode, the illuminated region can be controlled by Gaussian beam transforms by a set of lenses. However, for a focal plane array imaging system, it means that an object has a larger illuminating area accompanied with more serious distortions during wave propagation. In Figure 3, we compare the imaging results at 100 GHz, working at pixel scanning mode, focal plane array mode, and the simulation results from Fourier optics. The size of the object is $0.18 \times 0.18\,\mathrm{m}^2$ including both the gun and the background. The contrast between them is 9 dB, which corresponds to the case of metal and skin [4]. The periods of the random roughness are 8 wavelengths for the background and 4 wavelengths for the rough object. The maximum height difference of the object's surface is 1.5 mm. The diameter of the lens is 0.1 m for the scanning system and 1 m for the focal plane imaging system respectively. The focal distances are 0.2 m and 1 m respectively. The resolution is two wavelengths and the amplification ratio of the system is 1. We consider both the cases for smooth and rough objects with different roughness definitions.

As shown in Figure 3, for smooth objects, the imaging results are similar by applying all the three approaches. In case of rough objects, the pixel scanning system gives slightly worse results than the prediction by Fourier optics, while the focal plane array imaging system gives clearly the worst result. Among the three methods above, Fourier optics provides the best description of the object. To evaluate the image quality of the gun, we follow the concept of speckle contrast in [15], which is the deviation of the intensity divided by the average value. In Figure 3(e), the speckle contrast is 0.23, while the value is 0.18 in Figure 3(f). This means that by applying the focal plane array imaging approach, the difference in terms of speckle contrast is around 28% compared to the prediction by Fourier optics, which accounts for a more seriously blurred image. Note that in this case, even the diameter of the lens is more than five times' larger than the object, Fourier optics does not hold well. This obeys the conclusions in [14]. Focal plane array imaging is a very hot topic in millimeter wave imaging systems nowadays. However, before upgrading the scanning system, it should be clear that the focal plane imaging system is more than a parallel realization of pixel scanning systems and the image distortion is possibly much worse than the prediction by Fourier optics.

5. MATHEMATICAL ANALYSIS TO PREVIOUS RESULTS

In previous section, we have shown that for smooth objects, there is a good convergence for simulation results between Fourier optics and the method based on scalar diffraction in case of a smooth object; while for a rough object with a large illuminated area, the results attained by the two methods are quite different. Since Fourier optics can be considered as a simplified version of the method based on scalar diffraction, in this section, we will investigate the influence of the two procedures for simplification as follows, Fresnel approximation and the omission of the most important quadratic phase factor.

5.1. Influence of the Fresnel Approximation

Fresnel approximation is widely applied since it has a nice expression which can be calculated by Fourier transform. In this section, we will examine the effect that the Fresnel approximation has on wave

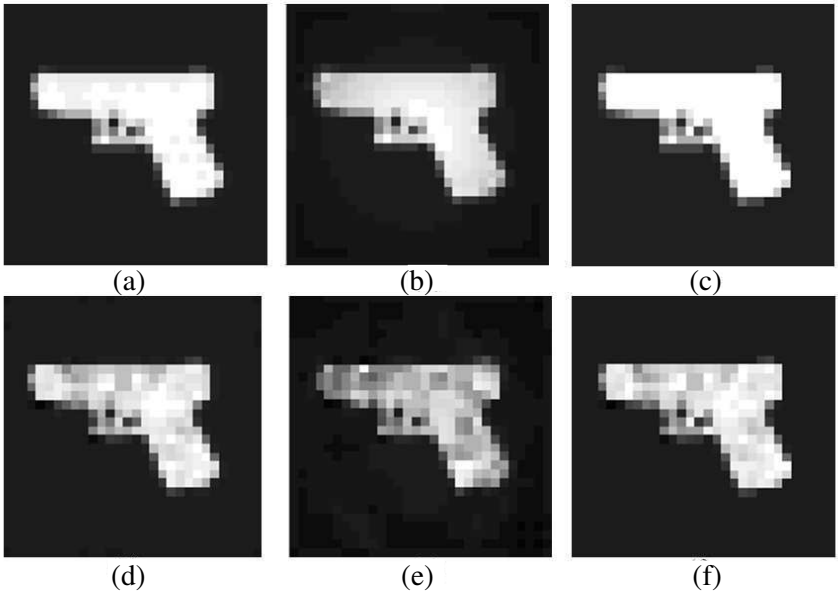

Figure 3. Comparison of different imaging approaches for a smooth and a rough object with random roughness. Upper row, smooth object; bottom row, rough object (a), (d) pixel scanning mode; (b), (e) focal plane array mode (c), (f) results predicted by Fourier optics.

propagation, which would influence the final image consequently. In [24], it is proved by numerical integrations that the Fresnel approximation is accurate even in extremely near field and phase errors are ignorable in the region of geometrical projection. The conclusions strongly promote that Fourier optics be valid at a much shorter distance. However, we should also pay attention to the fact that all the discussions on the accuracy of the Fresnel approximation, are limited to plane waves, without considering the phase shift of the wave source which can have high spatial-frequency components.

For simplicity, we only examine the influence of the phase factor, which is important to the integral values of formula (1). Mathematically, the diffraction formula can be expressed as (5), where k is the wave number, $g(x)$ stands for the amplitude distribution of the object field and $f(x)$ is the phase distribution of the object field divided by k plus the influence of propagated distance of the wave.

$$I = \int g(x)e^{jkf(x)}dx \tag{5}$$

According to the stationary phase theorem [25], if $g(x)$ changes slowly with the integral variable and k is a large number, the integral value can be determined mainly by the stationary phase points directly. Mathematically, the fast oscillations in phase between p and $-pi$ lead to the cancelation of the contributions from the amplitude distribution inside the integral. The key points are those who can make the first-order differential coefficient of the phase function to be equal to zero. In our discussion of the diffraction either in optics or in the millimeter wave region, it is suitable to apply the stationary phase analysis considering the small wavelengths with corresponding large wave numbers. Here x and x' represent the coordinates on the source and destination planes respectively. The distance between them is z. The overall phase function is expressed in (6), which is changed into (7) by making the Fresnel approximation. The letter "E" stands for "exact calculation", while the letter "F" stands for "Fresnel approximation".

$$f_E(x) = \phi(x)/k + z\sqrt{1 + [(x - x')/z]^2} \tag{6}$$

$$f_F(x) = \phi(x)/k + z + (x - x')^2/2z \tag{7}$$

To describe the object's spectrum, a simple sine function is assigned to phase in formula (8), where A stands for the amplitude of the height difference and T is the spatial period of the sine signal, and ω=$2\pi/T$. For general phase distributions, it is easy to expand the discussions by using a Fourier transform.

$$\phi(x) = kA\sin(\omega x) \tag{8}$$

Now the first-order derivatives can be expressed as (9) and (10), with $\Delta x = x - x'$. Both of them are functions of the offset along the x axis.

$$f'_E(x) = A\omega\cos(\omega x) + (1/z)\cdot\Delta x \Big/ \sqrt{1+(\Delta x/z)^2} \tag{9}$$

$$f'_F(x) = A\omega\cos(\omega x) + (1/z)\cdot\Delta x \tag{10}$$

In the following discussions, A is half a wavelength and we are interested at the distribution of the stationary phase points. So the calculation of the integral is in fact on how well the stationary phase points in formulas (9) and (10) can match. The periods of the phase shifts are 100 wavelengths and 5 wavelengths respectively. Here, we only show the case of the on-axis point on the destination plane. For off-axis points, we just need to move the curve to the left and right accordingly in Figure 4 and the difference between the two curves becomes larger. The distance between the source and the destination plane is 1 m. The intersection points between the curve and the horizontal line in the figure are the stationary phase points.

According to the results above, in case of a large period which represents a smooth object, the distributions of the stationary phase points are similar with and without Fresnel approximation. While as the spatial frequency increases, the amplitude of the differential function increases with a faster oscillation, as shown in Figures 4(c) and (d). There exists a case in which the number of stationary phase points would be clearly different by using or not the Fresnel approximation. In Figure 4(b), the Fresnel approximation implies around 10% loss of stationary points, resulting in a large difference between the values of the approximated and non-approximated integrals. Theoretically, the introduced phase errors by the Fresnel approximation are cumulative. As the frequency of the phase function increases, the number of stationary phase points may become larger as well, leading to possibly large errors in integral values. Moreover, the drastically increased number of stationary points would make the coupling between these points more significant. So, the Fresnel approximation may suffer from an obvious error when analyzing objects with high spatial frequency components. In this case, even in the geometrical projection region, the Fresnel approximation can not guarantee a good result, which obeys the conclusion of Southwell [24]. As discussed in Section Two, non-paraxial case is common in millimeter wave imaging systems, due to the small f-number of the lens, large field of view, large diffraction angle due to object's features with high spatial-frequencies and a small system scale. The Fresnel approximation, as the solution to paraxial Helmholtz equation, is not very accurate mathematically. From the Fourier transform point of view, Fraunhofer diffraction can

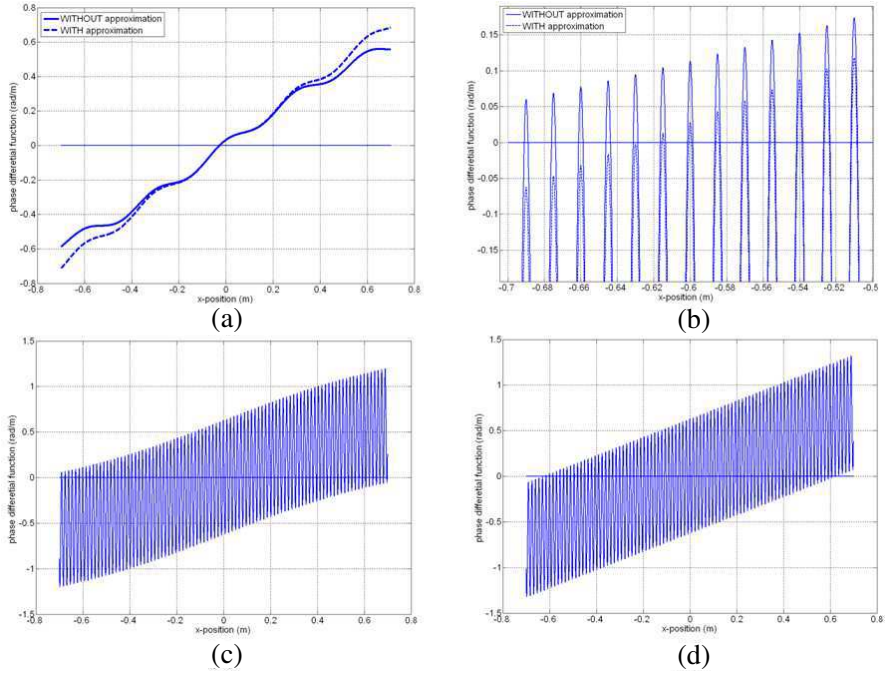

Figure 4. Comparison of the differential function of phase distribution for the on-axis point: WITH and WITHOUT approximation at $x' = 0$ (a) comparison of the stationary phase points $T = 100\lambda$; (b) comparison of the stationary phase points distribution $T = 5\lambda$, with an enlarged figure around the boundary in (c) and (d); (c) differential phase function $T = 5\lambda$, no Fresnel approximation; (d) differential phase function $T = 5\lambda$, with Fresnel approximation.

be considered as aberration free, Fresnel approximation introduces 2nd order aberration by deleting all the higher-order terms during expansion of the phase function. So in millimeter wave imaging systems, object's field is possibly distorted during wave propagation after a few meters due to diffraction. The purpose of optical system design is to decrease these aberrations introduced by the high-order terms. It is impossible to deal with all kinds of phase errors by a single lens. In many millimeter wave imaging systems, there is only one lens nowadays. Consequently, aberrations deserve our attention and the system is not as isoplanatic as the optical case. More lenses can be applied to improve the optical performance of the systems, however,

we should also consider the large losses at millimeter wave frequencies.

5.2. Influence of the Quadratic Phase Factor

In (3), there are five phase factors omitted by the Fourier relationship so as to realize mathematical simplicity. In [1], the conditions for the omission operation are discussed. The most important factor is $\exp(jk(\xi^2+\eta^2))$, since it interacts with the object field directly. Here, the interaction between the quadratic phase factor and the object field is examined. There are two questions: first, how large the difference between the integrals (11) and (12) can be; second, how the results are influenced by the spatial frequency of the object. We will analyze the questions in spatial-frequency domain, where formulas (13) and (14) are examined instead of formulas (11) and (12).

$$U_i(u) = \int P(x) \times \left[\int \left[U_o(\xi) e^{j\frac{k}{2z_1}\xi^2} \right] e^{-j\frac{2\pi}{\lambda z_1}x\xi} d\xi \right] \times e^{-j\frac{2\pi}{\lambda z_2}ux} dx \quad (11)$$

$$U_i(u) = \int P(x) \times \left[\int U_o(\xi) e^{-j\frac{2\pi}{\lambda z_1}x\xi} d\xi \right] \times e^{-j\frac{2\pi}{\lambda z_2}ux} dx \quad (12)$$

$$G_i(f_X) = H(f_X) F\{U(\xi) \times e^{jk\xi^2/2z_1}\} \quad (13)$$

$$G_i(f_X) = H(f_X) F\{U(\xi)\} \quad (14)$$

The quadratic phase factor in our case and its spectrum are shown in Figure 5. The spectrum is normalized and is shown in the range of $-250 \sim 250$ cycles per meter. Its bandwidth is considered to be 200 cycles per meter according to the power distribution of the spectrum. Both rough and smooth objects are investigated with and without the quadratic phase factor. The phase shift is the same as in previous discussion and the results are shown in Figure 6.

Here, we use the difference between the maximum and minimum amplitude divided by the average amplitude to evaluate the contrast of the image. As shown in Figures 6(a) and (b), for the smooth object, there is no obvious difference between the two images with and without multiplying the quadratic phase factor. Since the contrast is less than 2%, this situation is not sensitive to the difference. While in case of the rough object, two images are quite different, as shown in Figures 6(c) and (d). By taking the quadratic phase factor into account, the obtained image is not as uniform as the former one, which is quite regular and periodic. The contrast values are 1.5 and 1.8 respectively, corresponding to more than 20% difference. The irregularity in Figure 6(d) contributes to the distortion of the final image in reality.

The low-pass filtering effect of the imaging system is shown in Figure 7 for both the smooth and rough objects with and without the

quadratic phase factor. For the smooth object, by taking the quadratic phase factor into account, the spectrum is still in baseband, so that we get a smooth image correspondingly. For the rough object, the spectrum is quite different and a lot of new frequency components appear in the spatial frequency domain, resulting in different images.

Fourier analysis can be applied to analyze the results in Figure 7 The spectrum of the exponential function with a sine phase distribution is a set of pulses with a constant interval, which is proportional to the frequency of the sine signal in the spatial frequency domain. The spectrum manipulation by multiplying the quadratic phase factor can be understood as follows: first, the spectrum of the quadratic phase factor is weighted by the coefficient determined by the amplitude of the phase shift and Bessel functions, as shown in Figure 8; second, the weighted spectra are repeated at discrete spatial frequencies; third, interference happens to the overlapped spectra. The amplitude of the phase shift would influence the weighing factor and the corresponding spectrum, which can be analyzed according to the discussions above. The spatial truncation changes the pulse into a sinc function in transform domain.

To match the results in Figures 6 and 7, we will focus on the discussions at $x = pi$ and only examine the influence of the period of the phase function. However, the analysis can be generalized to other cases. The weighting factor is determined by the intersection points of Bessel function and $x = pi$. In Figures 7(c) and (d), the value for the peaks are according to the intersection points by $x = pi$ and 0, 1st, 2nd order Bessel functions. Moreover, the intersection points between $x = pi$ and higher-order Bessel functions have very small values, thus the result is mainly decided by the low-order Bessel

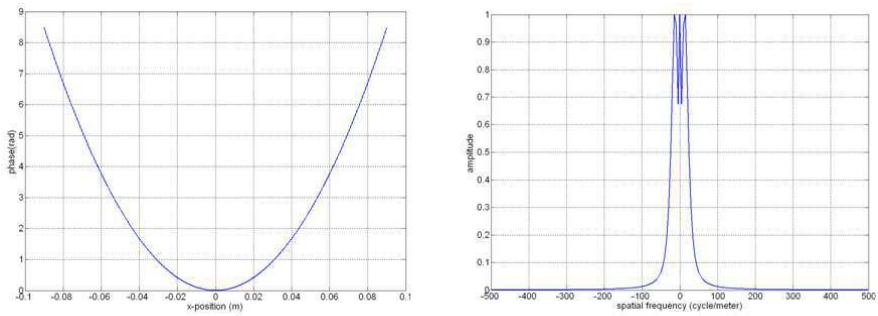

Figure 5. Quadratic phase factor and its spectrum, (a) in spatial domain; (b) in spatial frequency domain.

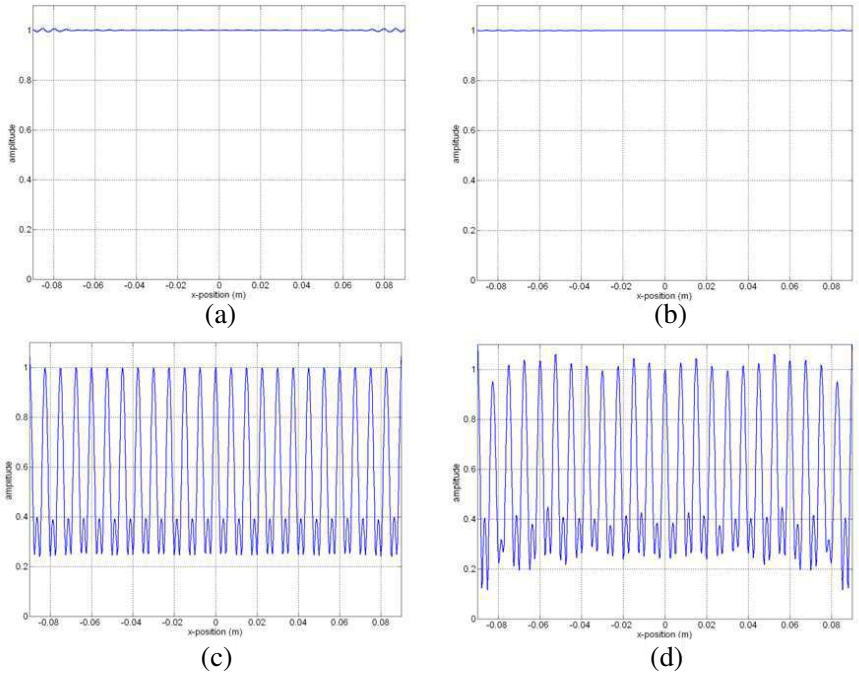

Figure 6. Influence of the quadratic phase factor on image (a) $T = 100\lambda$, without the quadratic phase factor. (b) $T = 100\lambda$, including the quadratic phase factor. (c) $T = 5\lambda$, without the quadratic phase factor. (d) $T = 5\lambda$, including the quadratic phase factor.

functions. When the period of the phase shift is 100 wavelengths, the pulses are very close to each other. Thus the repeated spectra after weighting interact with each other are still located in baseband. The narrower spectrum corresponds to a "flatter" image by including the quadratic phase factor. When the period of the phase shift is 5 wavelengths, the interval between pulses is expanded. In our case, the resultant spectrum has new spatial frequency components in a broader frequency range, which is shown in Figure 7(d). Moreover, interference between shifted spectra also contributes to some differences between the spectra with and without including the quadratic phase factor. The two points above account for the distortion in Figures 6(c) and (d).

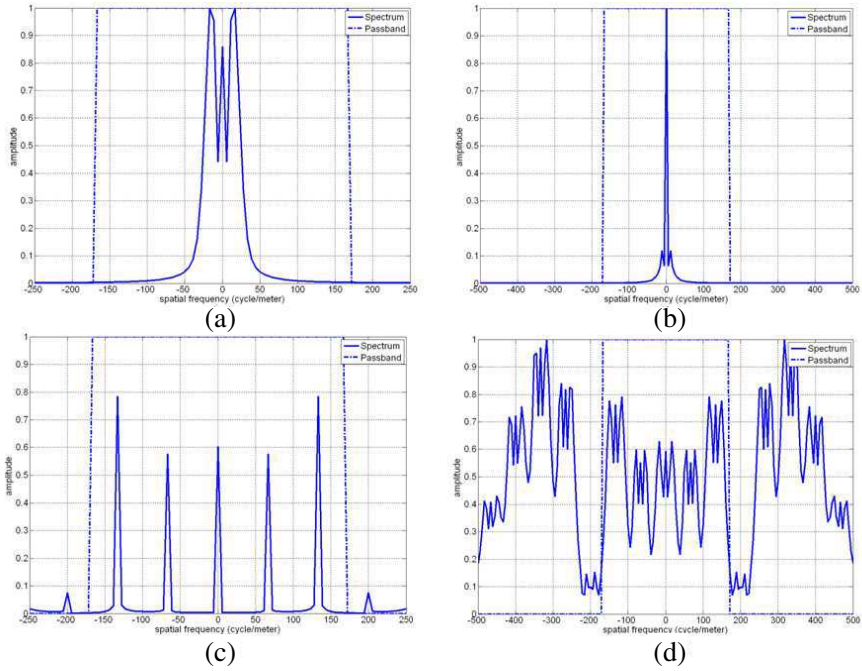

Figure 7. Influence of the quadratic phase factor on spectra (a) $T = 100\lambda$, without the quadratic phase factor, (b) $T = 100\lambda$, with the quadratic phase factor, (c) $T = 5\lambda$, without the quadratic phase factor, (d) $T = 5\lambda$, with the quadratic phase factor.

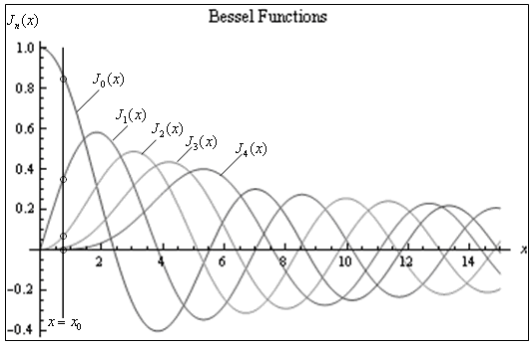

Figure 8. Determination of the weighting coefficient by Bessel function and the amplitude of the phase shift.

6. CONCLUSION

In this paper, we compare optical imaging systems and millimeter wave imaging systems. For the latter one, different imaging properties are discussed. The derivation process of the Fourier relationship between an object and its image is reviewed accompanied with a discussion on mathematical inaccuracies due to some approximations. The Fresnel approximation and omission of quadratic phase factors have assigned some limitations to this approach considering the practical non-paraxial case and possibly high spatial-frequency features of the object in millimeter wave imaging systems. By applying the stationary phase theorem, we validate the Fresnel approximation qualitatively. Based on spectrum analysis, we explain how the image is blurred due to the omission of the quadratic phase factor. Both of the two points above may break down the linear spatial invariant property of the imaging system. The analysis approaches can be generalized to a much wider range. To sum up, the method based on Rayleigh-Sommerfeld diffraction is accurate at the scale of scalar calculations. Direct application of Fourier optics forms the first-order approximation of the imaging system. Second-order approximation can be considered by including the phase factors omitted in Fourier optics. In practice, scanning imaging systems can be similar to the predictions by Fourier optics only if the scanning area is small enough.

REFERENCES

1. Goodman, J. W., *Introduction to Fourier Optics*, McGraw-Hill, 1996.
2. Kakimoto, M., K. Matsuoka, T. Nishita, and H. Harashima, "Glare generation based on wave optics," *12th Pacific Conference on Computer Graphics and Applications*, 133–142, 2004.
3. Flagello, D. G., T. Milster, and A. E. Rosenbluth, "Theory of high-NA imaging in homogeneous thin films," *J. Opt. Soc. Am*, Vol. 13, 53–64, 1996.
4. Goldsmith, P. R., C. T. Hsieh, G. R. Huguenin, J. Kapitzky, and E. L. Moore, "Focal plane imaging systems for millimeter wavelengths," *IEEE Trans. Microwave Theory and Tech.*, Vol. 41, 1664–1675, 1993.
5. Koers, G., I. Ocket, F. Qi, V. Tavakol, I. Jager, B. Nauwelaers, and J. Stiens, "Study of active millimeter-wave image speckle reduction by Hadamard phase pattern illumination," *J. Opt. Soc. Am A*, Vol. 25, 312–317, 2008.

6. Luo, Z., J. Xiong, and J. Yang, "A model-based analyzing and calculating of the focal plane array for passive millimeter wave imaging system," *International Conference on Communications, Circuits and Systems Proceedings*, 629–632, 2006.
7. Mezouari, S. and A. R. Harvey, "Validity of Fresnel and Franhofer approximations in scalar diffraction," *Journal of Optics A: Pure and Applied Optics*, 86–91, 2003.
8. Nauwelaers, B., I. Ocket, F. Qi, V. Tavakol, and D. Schreurs, "Is imaging with millimeter wave the same as optical imaging?" *Third European Conference on the Use of Modern Information and Communication Technologies*, 2008.
9. Thakur, J. P., W. G. Kim, and Y. H. Kim, "Large aperture low aberration aspheric dielectric lens antenna for W-band quasi-optics," *Progress In Electromagnetics Research*, Vol. 103, 57–65, 2010.
10. Dou, W. B., Z. L. Sun, and X. Q. Tan, "Fields in the focal space of symmetrical hyperbolic focusing lens," *Progress In Electromagnetics Research,* Vol. 20, 213–226, 1998.
11. Ghaffar, A. and Q. A. Naqvi, "Focusing of electromagnetic plane wave into uniaxial crystal by a three dimensional plano convex lens," *Progress In Electromagnetics Research*, Vol. 83, 25–42, 2008.
12. Ghaffar, A., A. A. Rizvi, and Q. A. Naqvi, "Fields in the focal space of symmetrical hyperboloidal focusing lens," *Progress In Electromagnetics Research,* Vol. 89, 255–273, 2009.
13. Rhodes, W. T., "Simple procedure for the analysis of coherent imaging systems," *Optics Letters*, Vol. 19, 1559–1561, 1994.
14. Tichenor, D. A. and J. W. Goodman, "Coherent transfer function," *J. Opt. Soc. Am*, 293–295, 1972.
15. Qi, F., V. Tavakol, D. Schreurs, and B. K. J. C. Nauwelaers, "Discussion on validity of hadamard speckle contrast reduction in coherent imaging system," *Progress In Electromagnetics Research*, Vol. 104, 125–143, 2010.
16. Hatamzadeh-Varmazyar, S., M. Naser-Moghadasi, and Z. Masouri, "A moment method simulation of electromagnetic scattering from conducting bodies," *Progress In Electromagnetics Research*, Vol. 81, 99–119, 2008.
17. Carpentieri, B., "Fast iterative solution methods in electromagnetic scattering," *Progress In Electromagnetics Research*, Vol. 79, 151–178, 2008.
18. Xin, Y. F. and P. L. Rui, "Adaptively accelerated GMRES fast fourier transform method for electromagnetic scattering," *Progress*

In Electromagnetics Research, Vol. 81, 303–314, 2008.

19. Du, Y., Y. Luo, W.-Z. Yan, and J. A. Kong, "An electromagnetic scattering model for soybean canopy," *Progress In Electromagnetics Research*, Vol. 79, 209–223, 2008.
20. Lin, Z., X. Zhang, and G. Fang, "Theoretical model of electromagnetic scattering from 3D multi-layer dielectric media with slightly rough surfaces," *Progress In Electromagnetics Research*, Vol. 96, 37–62, 2009.
21. Du, Y. and B. Liu, "A numerical method for electromagnetic scattering from dielectric rough surface based on the stochastic second degree method," *Progress In Electromagnetics Research*, Vol. 97, 327–342, 2009.
22. Faghihi, F. and H. Heydari, "Time domain physical optics for the higher-order FDTD modeling in electromagnetic scattering from 3-D complex and combined multiple materials objects," *Progress In Electromagnetics Research*, Vol. 95, 87–102, 2009.
23. Liang, D., P. Xu, L. Tsang, Z. Gui, and K.-S. Chen, "Electromagnetic scattering by rough surfaces with large heights and slopes with applications to microwave remote sensing of rough surface over layered media," *Progress In Electromagnetics Research*, Vol. 95, 199–218, 2009.
24. Southwell, W. H., "Validity of the Fresnel approximation in the near field," *J. Opt. Soc. Am*, Vol. 71, 7–14, 1981.
25. Born, M. and E. Wolf, *Principle of Fourier Optics*, Cambridge University Press, 1999.